Supplementary Materials for Fiber-based distributed sensing laser interferometer enabled by the mirror-image correlation method

1 Analysis of MI-correlation method in frequency domain

The fundamental nature of MI-correlation operation is to coherently enhance the signal component at the frequency $1/2\tau$. To explain it more clearly, the MI-correlation method is analyzed in frequency domain. Since $S_B(t)$ can be written as $S_B(t) = S_A(t+\tau_0)$, the frequency spectrum of the composite signal $S(t) = S_A(t) + S_B(t)$ can be calculated as follows:

$$\mathsf{F}(f) = \mathsf{F}_A(f) + \mathsf{F}_B(f) = \left(1 + e^{-j2\pi f\tau_0}\right)\mathsf{F}_A(f), \tag{S1}$$

where $\mathsf{F}_A(f)$ and $\mathsf{F}_B(f)$ are the frequency spectra of two original signals/vibrations $S_A(t)$ and $S_B(t)$. Therefore, the mirror-image steps in frequency domain are as follows:

1. Lag the initial signal $S(t)$ with τ, change its sign, and obtain the frequency spectrum of the 1st-order mirror signal:

$$\mathsf{F}_1(f) = (-1)^1 \cdot e^{-j2\pi f\tau} \cdot \mathsf{F}(f) = (-1)^1 \cdot e^{-j2\pi f\tau} \cdot \left(1 + e^{-j2\pi f\tau_0}\right)\mathsf{F}_A(f). \tag{S2}$$

2. Add $\mathsf{F}_1(f)$ to $\mathsf{F}(f)$ to obtain the frequency spectrum of the 1st-order output signal:

$$\mathsf{F}_{o1}(f) = \left[1 + (-1)^1 e^{-j2\pi f\tau}\right]\left(1 + e^{-j2\pi f\tau_0}\right)\mathsf{F}_A(f) = \frac{1-(-1)^2 e^{-j2\pi f2\tau}}{1+e^{-j2\pi f\tau}}\left(1 + e^{-j2\pi f\tau_0}\right)\mathsf{F}_A(f). \tag{S3}$$

3. Lag the 1st-order mirror signal $S_1(t)$ with τ, change its sign, and obtain the frequency spectrum of the 2nd-order mirror signal:

$$\mathsf{F}_2(f) = (-1)^1 \cdot e^{-j2\pi f\tau} \cdot \mathsf{F}_1(f) = (-1)^2 \cdot e^{-j2\pi f2\tau} \cdot \left(1 + e^{-j2\pi f\tau_0}\right)\mathsf{F}_A(f). \tag{S4}$$

4. Add $\mathsf{F}_2(f)$ to $\mathsf{F}_{o1}(f)$ to obtain the frequency spectrum of the 2nd-order output signal:

$$\mathsf{F}_{o2}(f) = \left[1 + (-1)^1 e^{-j2\pi f\tau} + (-1)^2 e^{-j2\pi f2\tau}\right]\left(1 + e^{-j2\pi f\tau_0}\right)\mathsf{F}_A(f) = \frac{1-(-1)^3 e^{-j2\pi f3\tau}}{1+e^{-j2\pi f\tau}}\left(1 + e^{-j2\pi f\tau_0}\right)\mathsf{F}_A(f). \tag{S5}$$

By repeating steps 1–4, for the ith-order mirror-image step, we can write the frequency spectrum of the ith-order mirror signal $S_i(t)$ as $\mathsf{F}_i(f) = (-1)^i \cdot e^{-j2\pi fi\tau} \cdot \left(1 + e^{-j2\pi f\tau_0}\right)\mathsf{F}_A(f)$. Add $\mathsf{F}_i(f)$

to $\mathrm{F}_{o(i-1)}(f)$ to obtain the frequency spectrum of the ith-order output signal $\mathrm{F}_{oi}(f)=\frac{1-(-1)^{i+1}e^{-j2\pi f(i+1)\tau}}{1+e^{-j2\pi f\tau}}\left(1+e^{-j2\pi f\tau_0}\right)\mathrm{F}_A(f)$. After m times mirror-image operations, we obtain the frequency spectrum of the mth-order output signal, which can be written as:

$$\mathrm{F}_{om}(f)=\frac{1-(-1)^{m+1}e^{-j2\pi f(m+1)\tau}}{1+e^{-j2\pi f\tau}}\left(1+e^{-j2\pi f\tau_0}\right)\mathrm{F}_A(f). \tag{S6}$$

When m is chosen as even number, we can conclude that:

$$\begin{aligned}\left|\mathrm{F}_{om}(f)\right| &= \frac{\left|1+e^{-j2\pi f(m+1)\tau}\right|}{\left|1+e^{-j2\pi f\tau}\right|}\cdot\left|1+e^{-j2\pi f\tau_0}\right|\cdot\left|\mathrm{F}_A(f)\right| \\ &= \sqrt{\frac{2+2\cos\left[2\pi f(m+1)\tau\right]}{2+2\cos(2\pi f\tau)}\left[2+2\cos(2\pi f\tau_0)\right]}\cdot\left|\mathrm{F}_A(f)\right|\end{aligned}, \tag{S7}$$

where $\sqrt{\frac{2+2\cos\left[2\pi f(m+1)\tau\right]}{2+2\cos(2\pi f\tau)}}$ is the amplification factor of original spectrum. When $f=1/2\tau$, it reaches the maximum value of m+1, that is, $\left|\mathrm{F}_{om}(\frac{1}{2\tau})\right|=(m+1)\sqrt{\left[2+2\cos\left(\pi\frac{\tau_0}{\tau}\right)\right]}\cdot\left|\mathrm{F}_A(\frac{1}{2\tau})\right|$. When the estimated time delay is $\tau=\tau_0$, $\sqrt{2+2\cos\left(\frac{\tau_0}{\tau}\pi\right)}=0$ is achieved, the induced mark error is zero. In other cases, the signal component at the frequency $1/2\tau$ is amplified by m+1 times.

2 Effect of MI-correlation method in time domain

Based on $\left|\mathrm{F}_{om}(\frac{1}{2\tau})\right|=(m+1)\sqrt{2+2\cos\left(\frac{\tau_0}{\tau}\pi\right)}\cdot\left|\mathrm{F}_A(\frac{1}{2\tau})\right|$, it can be concluded that if $\left|\mathrm{F}_A(\frac{1}{2\tau})\right|=0$, the result for $\left|\mathrm{F}_{om}(\frac{1}{2\tau})\right|$ will always be 0 regardless of the value of τ. That is to say, the Sagnac interferometry (SI) based positioning techniques and the MI-correlation method both require that the spectrum should be broad, otherwise they can't work well. In reality, most of the measured vibration signals are non-stationary and vary in frequency over time. Their broad-spectrum

components may have a very short duration, for example, occurring only within a few milliseconds when a sudden vibration occurs. The short duration of the broad-spectrum signal makes it difficult to achieve high resolution in frequency domain analysis. Increasing the length of the analyzed signal will deteriorate the signal-to-noise ratio (SNR) because it introduces too many useless signal segments. It presents a significant challenge for SI based positioning techniques that relies on frequency-dependent zero points. However, for the MI-correlation method, there is no requirement for the duration of the broad-spectrum components of the vibration signal. Even broad-spectrum components with a very short duration can be captured by the method and used for time delay estimation. To clarify its ability, the MI-correlation method is analyzed in time domain.

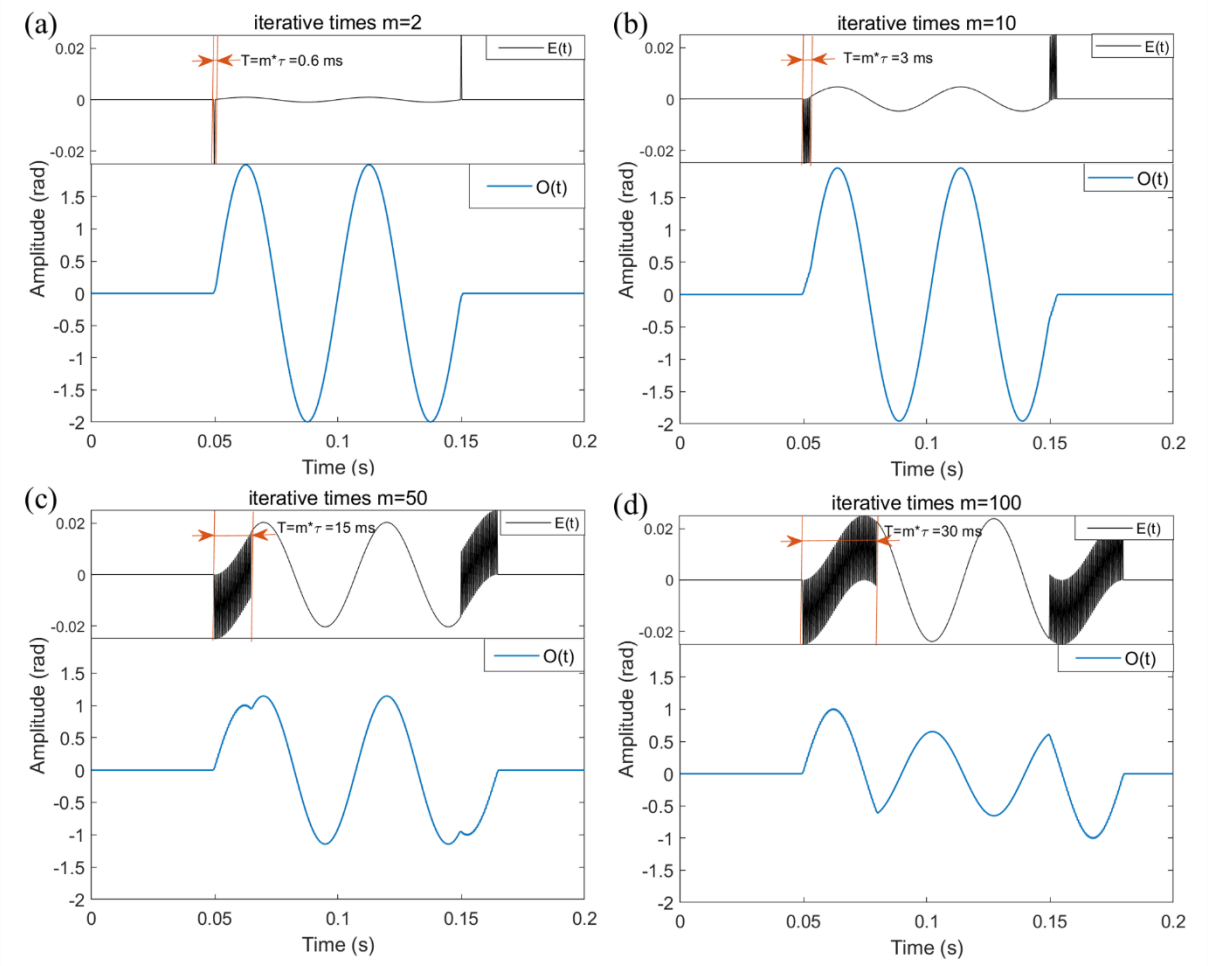

Fig. S1. The effect of MI-correlation method in time domain. (a), (b), (c) and (d) The output signal $O(t)$. and the mark error $E(t)$ at m=2, m=10, m=50 and m=100 mirror-image operations. The duration of frequency-controllable error marks T always satisfy $T = m\tau$.

To show the detailed MI-correlation process and demonstrate its feasibility, a 20 Hz sinusoidal signal is used for simulation. The time delay τ_0 between parts $S_A(t)$ and $S_B(t)$ is 500 μs. They overlap with each other and cannot be distinguished. The operation similar to that described in Section 3.1 is applied. A wrong time delay $\tau = 300$ μs is chosen in this demonstration. After mirror-image operations, the output signal $O(t)$ can be obtained. The result at m=2, m=10, m=50 and m=100 mirror-image operations are shown in Figs. S1(a)-(d), respectively. In the simulation, the original signal $S_A(t)$ can be obtained easily, thus the mark error $E(t)$ can be calculated by $E(t) = O(t) - \left[S_A(t) + (-1)^m S_A(t + \tau_0 + m\tau) \right]$, which are shown in the small windows in Figs. S1(a)-(d).

The MI-correlation method achieves time delay estimation by introducing a frequency-controllable error mark. The duration of the error mark depends not only on the duration of the broad-spectrum components but also on the number of mirror-image operations. For the simulated signal of 20 Hz, only its beginning and ending segments will have a complex spectral composition and response to the MI-correlation method. Therefore, for the mark error $E(t)$ in Fig. S1, it can be found that the frequency-controllable error marks appears only at the beginning and ending of the vibration signal, and its duration T always satisfy $T = m\tau$. It proves that the MI-correlation method not only enhances the component with the frequency of $1/2\tau$ in the frequency domain but also extends the duration of this frequency component in the time domain. It is a significant advantage of the MI-correlation method to capture transient broad-spectrum components in the signal and use them for time delay estimation.

3 Comparison between MI-correlation method and SI based positioning techniques that directly detect the zero point.

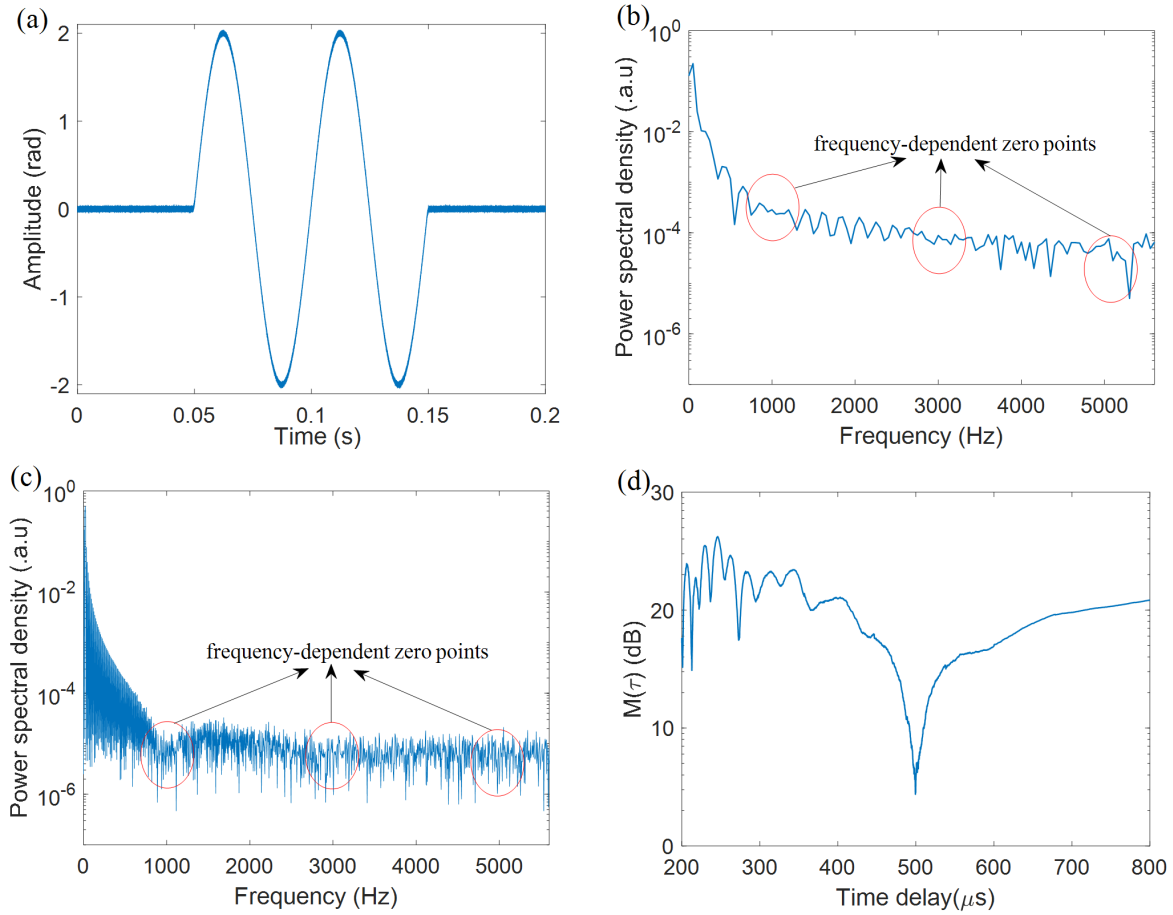

Fig. S2. The comparison between MI-correlation method and SI based positioning techniques that directly detect the zero point. (a) The 20Hz signal with 20dB white noise. (b) The frequency spectrum of the 20Hz signal with resolution of 100Hz. (c) The frequency spectrum of the 20 Hz signal with resolution of 5Hz. (d) MI-correlation indicator $M(\tau)$ of the 20 Hz signal. The true time delay of $\tau_0 = 500$ μs is obtained.

The influence of the MI-correlation method on the time domain makes it suitable for accurate time delay estimation of non-stationary vibration signals. To compare the MI-correlation method and SI based positioning techniques that directly detect the zero points, we conduct a simulation by adding 20dB white noise to the 20Hz signal, the composite signal $S(t)$ is shown in Fig. S2(a).

The frequency spectrum of the signal from 0.045 s to 0.055 s and the signal from 0 to 0.2 s are shown in Fig. S2(b) and Fig. S2(c), respectively. In Fig. S2(b), due to the short signal length, the frequency domain resolution is limited to 100 Hz, making it impossible to obtain frequency-dependent zero points. For the signal from 0 to 0.2 s, it includes longer signal segments that do not contain high-frequency components, the SNR deteriorates. In Fig. S2(c), the frequency-dependent zero points are affected by noise, making accurate observation difficult. In contrast, MI-correlation method can extend the duration of broad-spectrum signal from an instant to more than 10 ms. It helps to better analyze the signal effectively and achieve more accurate time delay estimation. The result is shown in Fig. S2(d) and the real time delay 500 μs can be obtained.

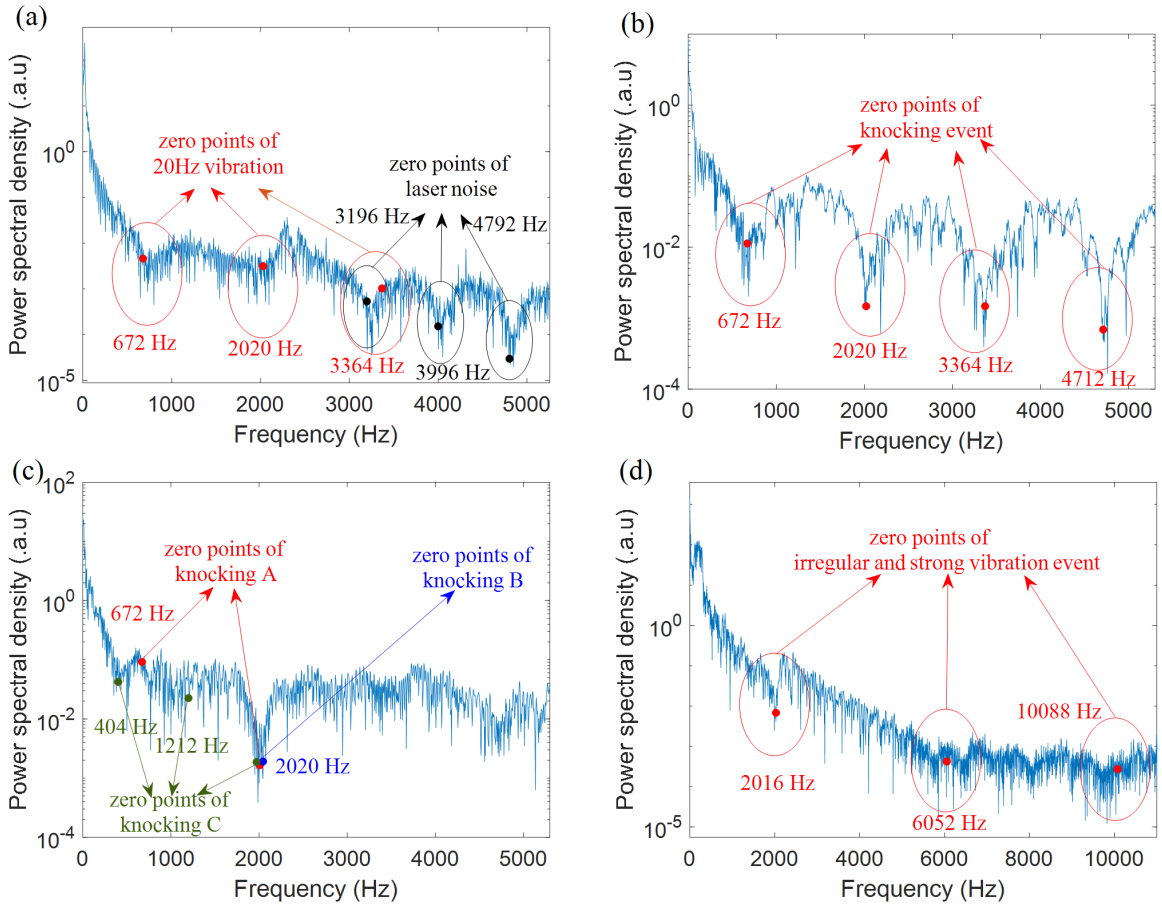

Fig. S3. The experiments of the SI based positioning techniques that directly detect the zero point. (a) The frequency spectrum of the 20 Hz vibration event. (b) The frequency spectrum of the knocking events at point A. (c) The frequency spectrum of the knocking events occurring simultaneously at points A, B and C. (d) The frequency spectrum of the irregular and strong vibration occurring at point B.

Furthermore, in the main text, multiple experiments are conducted to demonstrate the effectiveness of using the MI-correlation method for vibration positioning. In subsequent demonstrations, the same experimental data is used to analyze the SI based positioning techniques that directly detect the zero point.

First, the vibration event with the frequency of 20 Hz, as illustrated in Fig. 3(b) of Section 3.1, is used for demonstration. The frequency spectrum of this signal from 0.17 s to 0.42 s is shown in Fig. S3(a). For this vibration, the time delay τ_0 between parts $S_A(t)$ and $S_B(t)$ is $\tau_0 = 743\,\mu s$. Therefore, its first to third zero points are 673 Hz, 2019 Hz, and 3365 Hz, respectively. They are shown in Fig. S3(a), and it is evident that they are severely affected by noise, making it difficult to achieve accurate vibration positioning using them. Points with frequencies higher than the third zero point are covered by the laser noise, which exhibit the characteristics associated with the noise of an unequal-arm interferometer.

Second, the knocking events at point A, as illustrated in Fig. 5(a) of Section 3.3, are used for demonstration. The frequency spectrum of this signal from 1.2 s to 1.45 s is shown in Fig. S3(b). The first to forth zero points of this vibration are 673 Hz, 2019 Hz, 3365 Hz and 4711 Hz, respectively. They are shown in Fig. S3(b), where the zero points are obvious, indicating the potential for use in vibration positioning. It is because the 20 Hz signal contains only minor broad-spectrum components at the beginning and ending, making spectral analysis seriously affected by noise. In contrast, the broad-spectrum components in the knocking signal last longer, resulting in a better SNR compared to the 20 Hz signal.

Third, we analyze the knocking events occurring simultaneously at points A, B and C, as illustrated in Fig. 5(c) of Section 3.3. The frequency spectrum of this signal from 0 to 0.25 s is shown in Fig. S3(c). The first and second zero points of knocking A are 673 Hz and 2019 Hz. The first zero point of knocking B is 2018 Hz. The first to third zero points of knocking C are 404 Hz, 1212 Hz and 2020 Hz. They are shown in Fig. S3(c). The common zero point for these three knocking events(~2020Hz) is obvious, while the other points are quite chaotic. The mutual interference among three knocking events makes it difficult to simultaneously localize these three vibrations.

Finally, we analyze the irregular and strong vibration occurring at point B, as illustrated in Fig. 7(a) of Section 4. With the help of MI-correlation method, we can localize it. The standard deviation of the localization results is 17.6 m. The frequency spectrum of this signal from 0.95 s to 1.2 s is shown in Fig. S3(d). For this vibration, the time delay τ_0 between parts $S_A(t)$ and $S_B(t)$ is $\tau_0 = 248$ μs. Therefore, its first to third zero points of this vibration are 2018 Hz, 6053 Hz and 10088 Hz, respectively. They are shown in Fig. S3(d). Only the first zero point can be observed, while the other zero points hardly exhibit the corresponding characteristics, making it difficult to directly use the frequency spectrum for localization.

Overall, of the various scenarios mentioned in the main text that can utilize the MI-correlation method for distributed vibration localization, only a part of them can be located by directly detecting the zero points. When the duration of broad-spectrum vibration is short, such as transient excitation, the MI-correlation method offers better localization function than SI based positioning techniques that directly detect the zero point.